Asian Journal of Chemistry; Vol. 31, No. 12 (2019), 2785-2792

ASIAN JOURNAL OF CHEMISTRY

https://doi.org/10.14233/ajchem.2019.22213

Synthesis and Characterization of Magnetic Fe_3O_4/Reduced Graphene Oxide and its Application in Determination of Dopamine

A.R. ROSLI, S.H. LOH and F. YUSOFF*

Faculty of Science and Marine Environment, Universiti Malaysia Terengganu, 21030, Kuala Nerus, Terengganu, Malaysia

*Corresponding author: Fax: +60 9 6683193; Tel: +60 9 6683804; E-mail: farhanini@umt.edu.my

Received: 26 May 2019; *Accepted*: 10 July 2019; *Published online*: 16 November 2019; AJC-19620

An electrochemical sensor to determine dopamine in the human body was fabricated based on modified iron oxide/reduced graphene oxide/glassy carbon electrode (Fe_3O_4/r-GO/GCE). Determination of dopamine is significance nowadays as the abnormal level may cause various mental health diseases as well as Parkinson's disease. The Fe_3O_4/r-GO nanocomposite was synthesized *via* Hummer's method with a slight modification and characterized by Fourier transform infrared (FTIR), scanning electron microscopy (SEM), X-ray diffraction (XRD) and Brunauer Emmett-Teller (BET). The presence of Fe_3O_4 onto the surface of r-GO was confirmed by SEM analysis which shows the bulky porous sponge-like structure attached to an exfoliated sheet of r-GO. FTIR analysis proved the presence of the functional group in existing composites *via* oxidation process of graphene oxide and reduction process of reduced graphene oxide while the crystalline form of Fe_3O_4/r-GO was determined using XRD analysis. The diffraction peaks index to the cubic phase was noticeable indicating the successful crystallization of the composites. The catalytic activity of bare GCE and modified GCE (Fe_3O_4/r-GO/GCE) were observed using electrochemical characterization of cyclic voltammetry, differential pulse voltammetry (DPV) and electrochemical impedance spectroscopy (EIS) with optimum pH of 7, a concentration of 100 µM, and the scan rate of 250 mV s^{-1}. The observed DPV response linearly depends on dopamine concentration in the range of 20-100 µM, with correlation coefficients of 0.9876. The detection limit obtained for the real sample analysis was found to be 0.569 µM while the limit of quantitation was 1.897 µM. The percentage of recovery, repeatability and reproducibility was 113, 82.81 and 7.19 %, respectively.

Keywords: Graphene, Magnetite, Electrochemical sensor, Dopamine.

INTRODUCTION

Dopamine is a distinctive neurotransmitter, a chemical released by nerve cells to send information to other neurons and it plays a crucial role in brain and outside the central nervous system. Dopamine is extensively distributed in the cardiovascular systems, hormonal and memory and acts as a unique neurotransmitter that possesses the inhibitory and exhibitory behaviours [1]. Inhibitory neurotransmitter reposes the brain while the agitation of the brain is caused by the exhibitory neurotransmitter [2]. Dopamine is a small biomolecule and often present in biological matrices and commonly detected in urine, blood or high concentration of extracellular fluid in the body [3]. To date, several advanced analytical methods with excellent sensitivity and selectivity have been discovered for detecting dopamine in biological samples. However, the best alternative for sensing of dopamine is by using an electrochemical method as this technique offer a green approach, cost-effective and at the same time has high sensitivity.

Recently, graphene has captivated potent scientific and technological interest due to its specific physicochemical properties which are high surface area (theoretically 2630 m^2 g^{-1} for single-layer graphene), good thermal and electric conductivity and stable mechanical strength [2]. Graphene has shown a great performance in electroanalysis which is a chemical sensor and biosensor. Functionalized graphene sheets or known as chemically reduced graphene oxide (c-rGO) where it is reduced from graphite oxide usually has sufficient functional groups and structural defects which are very favourable for electrochemical applications [4]. According to Zhou *et al.* [5], graphene displays an extensive electrochemical potential window of about 2.5 V in 0.1 M phosphate buffer solution with pH 7. The charge-transfer resistance of graphene from alternating current impedance spectra (ACIS) is much lower than graphite

and glassy carbon electrode which made graphene is as good as glassy carbon, graphite and boron doped diamond electrode [5].

Iron oxide nanoparticles (Fe_3O_4) or also known as magnetite possess excellent magnetic properties, is a biocompatible material which is suitable for the sensing of biological analyte *e.g.*, dopamine, uric acid and ascorbic acid. Magnetite shows a superparamagnetism phenomenon wherein the external magnetic field application, the nanoparticles become saturation magnetization, and they no longer show any residual magnetic interaction upon removal of the magnetic field [6]. With the particles of small size, magnetite does not show the multiple domains were commonly found in the large magnets.

However, magnetite becomes a single magnetic domain and serves as 'single super spin' that display an exquisite magnetic sensitivity [7]. Therefore, magnetite is a suitable particle that can be used for the sensing of dopamine but magnetite itself is not so compromising due to its unstable properties and tendency to oxidize to other forms thus, graphene based magnetite nanoparticles are ideal for the improvement of an electrochemical sensor.

EXPERIMENTAL

Natural graphite powder, sodium nitrate, conc. sulfuric acid (95-98 %), potassium permanganate, hydrogen peroxide (30 %), hydrochloric acid (5 %), ammonium hydroxide, ammonia (30 %) and aluminium oxide was purchased from Merck, USA. Ferric chloride, ferrous chloride and hydrazine hydrate were purchased from R&M Chemicals. Phosphate buffer solution which acts as supporting electrolyte was prepared by mixing potassium dihydrogen phosphate and dipotassium hydrogen phosphate that was purchased from Sigma Aldrich, USA.

The electrochemical testing was performed by using a 3-electrode system consist of platinum wire that act as auxiliary electrode, reference electrode of Ag/AgCl electrode (Methrom, with 3M of KCl) and glassy carbon electrode (BASi MF-2012 3.0 mm diameter), with or without modification of Fe_3O_4/rGO as working electrode with use of Potentiostat/Galvanostat module PGSTAT (Metrothm AUTOLAB, Netherlands). Characterizations of unmodified or modified glassy carbon electrode were analyzed using Fourier transform infrared (FTIR, Perkin-Elmer Spectrum 100), scanning electron microscopy (SEM, JSM-6360, LA), X-ray diffraction (XRD, Rigaku MiniFlex II) and electrochemical impedence spectroscopy.

Synthesis of magnetic Fe_3O_4/rGO nanocomposites: Firstly, graphene oxide (GO) was synthesized *via* Hummer's method with slight modification [8,9]. The obtained 1 g GO was dispersed in distilled water using sonicator for about 0.5 h and labeled as solution **1**. $FeCl_3 \cdot 6H_2O$ and $FeCl_2 \cdot 4H_2O$ with molar ratio 2:1 were dissolved in distilled water and labeled as solution **2**. Solution **2** was then being added slowly to solution 1 under controlled temperature and a base solution (NaOH solution) was then added to make the pH of solution basic (pH 10). Hydrazine hydrate that acts as reducing agent to reduce the GO to reduced graphene oxide (rGO) was added with an elevation of temperature upto 85-90 ºC and under constant stirring condition. The black coloured precipitate was then washed with deionized water and ethanol to neutralize the pH and dried to obtain a black powdered Fe_3O_4/rGO nanocomposite.

Fabrication of Fe_3O_4/rGO/GCE: One spatula of alumina powder was mixed with several drops of deionized water and glassy carbon electrode was polished and rinsed with the slurry alumina powder. The GCE were then immersed in ethanol and distilled water and sonicated for about 10 min to remove the adsorbed particles on electrode. The Fe_3O_4/ rGO powder (10 mg) were then dissolved with 10 mL deionized water and sonicate for 10 minutes to obtain a homogeneous solution of Fe_3O_4/ rGO suspension to be drop-cast on top of the GCE surface. At least 7 µL of Fe_3O_4/ rGO suspension was cast onto the GCE.

Physical and electrochemical characterization of Fe_3O_4/ rGO/GCE: Glassy carbon electrode with or without modification of Fe_3O_4/ rGO were characterized physically using FTIR, SEM, XRD and BET. The functional group presence in graphite, graphene oxide, iron oxide and iron oxide/reduced graphene oxide were determined through FTIR while the surface morphology of graphite, graphene oxide, reduced graphene oxide, iron oxide and iron oxide/reduced graphene oxide were obtained from SEM test and identification of crystalline material of graphite, GO, rGO, Fe_3O_4 and Fe_3O_4/rGO were identified by XRD.

Electrochemical characterization using cyclic voltammetry and differential pulse voltammetry techniques were used to determine the desired voltage and current to find the best peak separation and diffusion coefficient among the modified GCE. Three electrode systems with modified glassy carbon electrode as the working electrode, platinum wire that act as the auxiliary electrode and reference electrode of Ag/AgCl electrode was used for the analysis. Supporting electrolyte of 1.0 mol of KCl and 5.0 mmol of potassium ferrocyanide were used with scan rate of 150 mV s^{-1} and 6 number of scans. The potential range is from – 0.2 V to 0.8 V.

Determination of dopamine in real samples: The urine excreted through human body was used for real sample as the dopamine is most likely to excrete through urine. The real sample was used to determine the content of dopamine from different individual using spiked solution, relative recovery study, repeatability and reproducibility, limit of detection and limit of quantification. The minimal conditions of those validations are important so that even low concentration of dopamine can be detected. Cyclic voltammetry and differential pulse voltammetry were used to obtain the oxidation peak of dopamine through voltammograms. The voltammogram analyses were then used to plot a calibration curve and the analysis were used as an indicator to determine the concentration of dopamine in urine sample.

RESULTS AND DISCUSSION

Physical characterization of Fe_3O_4/rGO nanocomposites: The use of FTIR in physical characterization of composite is to determine the presence of functional groups in graphite, graphene oxide, iron oxide and iron oxide/reduced graphene oxide. FTIR spectra of graphite (Fig. 1) show no significant peaks which indicate the graphite purity as well as acted as the background [10]. FTIR spectra of GO with peaks of O-H stretch, C=O carbonyl stretching, C=C aromatic stretching, C-H bend, C-OH stretching and C-O epoxy stretching are shown by the characteristic peaks at 3421, 1718, 1626, 1398, 1227 and 1080 cm^{-1}, respectively. Due to the wet synthesis of iron oxide using abundance usage of water, the peak of O-H stretches

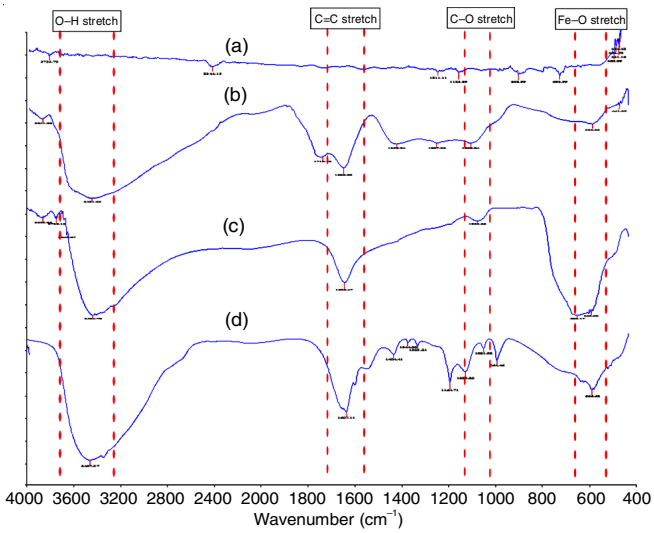

Fig. 1. FTIR spectra of (a) graphite, (b) GO, (c) Fe_3O_4 and (d) Fe_3O_4/rGO

at 3424 cm^{-1}, C=C stretch at 1626 cm^{-1} and C-O stretch at 1053 cm^{-1} show their peak in the spectrum. Hence, based on the desired peak obtained from the FTIR analysis, it can be concluded that Fe_3O_4/rGO have been successfully synthesized.

XRD analysis gives information about the crystalline components present in the composites, which are important to justify the complete synthesization of Fe_3O_4/rGO composite. The XRD spectra of graphite, GO, r-GO, Fe_3O_4 and Fe_3O_4/rGO are shown in Fig. 2. The Fe_3O_4/rGO peak at $2\theta = 18.53°$, 35.54°, 43.34°, 53.69°, 57.09°, 62.81° and 74.09° display that the peak of Fe_3O_4 remained and this proves that Fe_3O_4 is not reduced by the electrochemical reduction. The peak at 24.41° is disappeared indicating that the rGO is fully covered by iron oxide nanoparticles and this can also be proved through the SEM micrograph discussed later. Based on the crystallite size calculated, Fe_3O_4/rGO gives a highest crystallite size (112.99 Å) compared to GO, rGO, and Fe_3O_4 which give value of 66.59, 23.28 and 85.97 Å, respectively. The value of crystallite size is chosen from the highest peak of XRD diffractogram (Fig. 2).

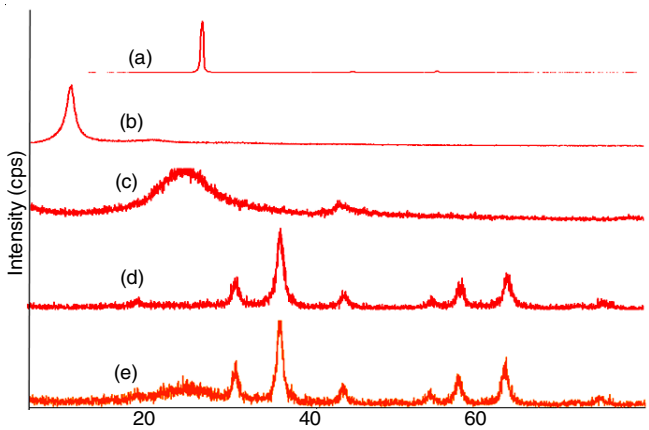

Fig. 2. XRD diffractogram of (a) graphite, (b) GO, (c) rGO, (d) Fe_3O_4 and (e) Fe_3O_4/rGO

SEM analysis is widely used to identify the external morphology (texture) of the composite Fe_3O_4/rGO. Fig. 3 shows the morphology of graphite (a), GO (b), rGO (c), Fe_3O_4 (d) and Fe_3O_4/rGO (e). The formation of Fe_3O_4/rGO is confirmed by SEM image (e) which shows the sphere-shaped structure of Fe_3O_4 attached to a layer of exfoliated rGO indicating that rGO is successfully covered with Fe_3O_4 nanoparticles. The average particle size of Fe_3O_4 in Fe_3O_4/rGO nanocomposite is smaller than Fe_3O_4 itself, indicating that the addition of rGO has suppressed the crystal growth of Fe_3O_4 to some extent [11].

BET technique includes external area and pore area evaluations to determine the total specific surface area in m^2/g yielding important information in studying the effects of surface porosity and particle size. BET is used to prove the hypothesis from SEM micrograph which shows the Fe_3O_4 nanoparticles being attached to the rGO surface by the surface area of composite.

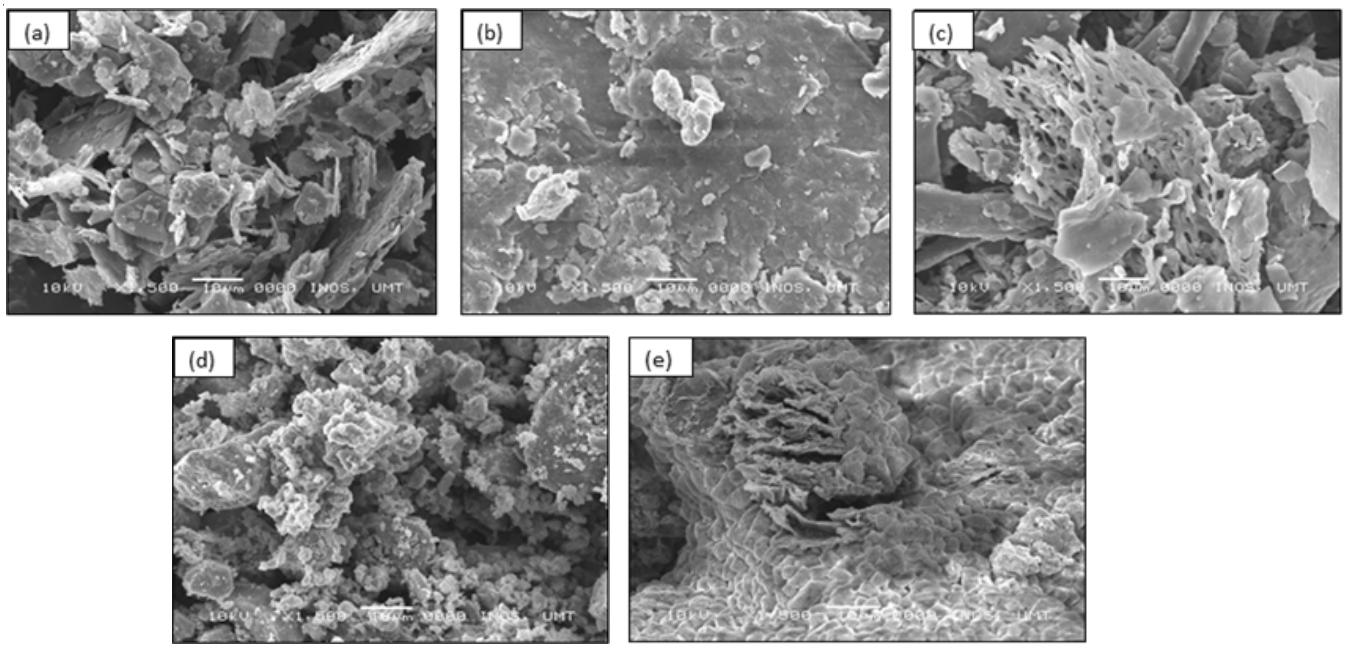

Fig. 3. SEM micrographs of (a) graphite, (b) GO, (c) rGO, (d) Fe_3O_4, and (e) Fe_3O_4/rGO with magnification of x1500 and the operational voltage of 10 kV

The BET surface area, Langmuir surface area, pore volume and pore size values of five samples of graphite, GO, rGO, Fe_3O_4 and Fe_3O_4/rGO are given in Table-1.

TABLE-1
INFORMATION OBTAINED FOR BET ANALYSIS

	BET surface area (m^2/g)	Langmuir surface area (m^2/g)	Pore volume (cm^3/g)	Pore size (nm)
Graphite	11.1987	15.4923	0.0430	15.374
GO	408.5683	545.7863	1.9817	19.402
rGO	39.6341	61.1224	0.2305	23.266
Fe_3O_4	114.1516	160.0887	0.3833	13.431
Fe_3O_4/rGO	109.3246	153.5981	0.2943	10.769

Fig. 4 shows the N_2 isotherm adsorption linear plot for graphite, GO, rGO, Fe_3O_4 and Fe_3O_4/rGO. Based on the figures, all the composites show a characteristic of Type IV isotherm which is the hysteresis loop (IUPAC) where these types of graph exhibit the capillary condensation taking place in mesopores [12]. The shapes of the hysteresis loop can classify the specific pore structure. Graphite and GO exhibit the H_2 loop which the pores structure is being said to be pores with narrow necks and wide-bodies while rGO, Fe_3O_4 and Fe_3O_4/rGO display a H3 loop which observed with aggregates of plate-like particles giving rise to slit-shaped pores.

Electrochemical characterization of Fe_3O_4/rGO nanocomposite: The electrochemical behavior of the electrode was

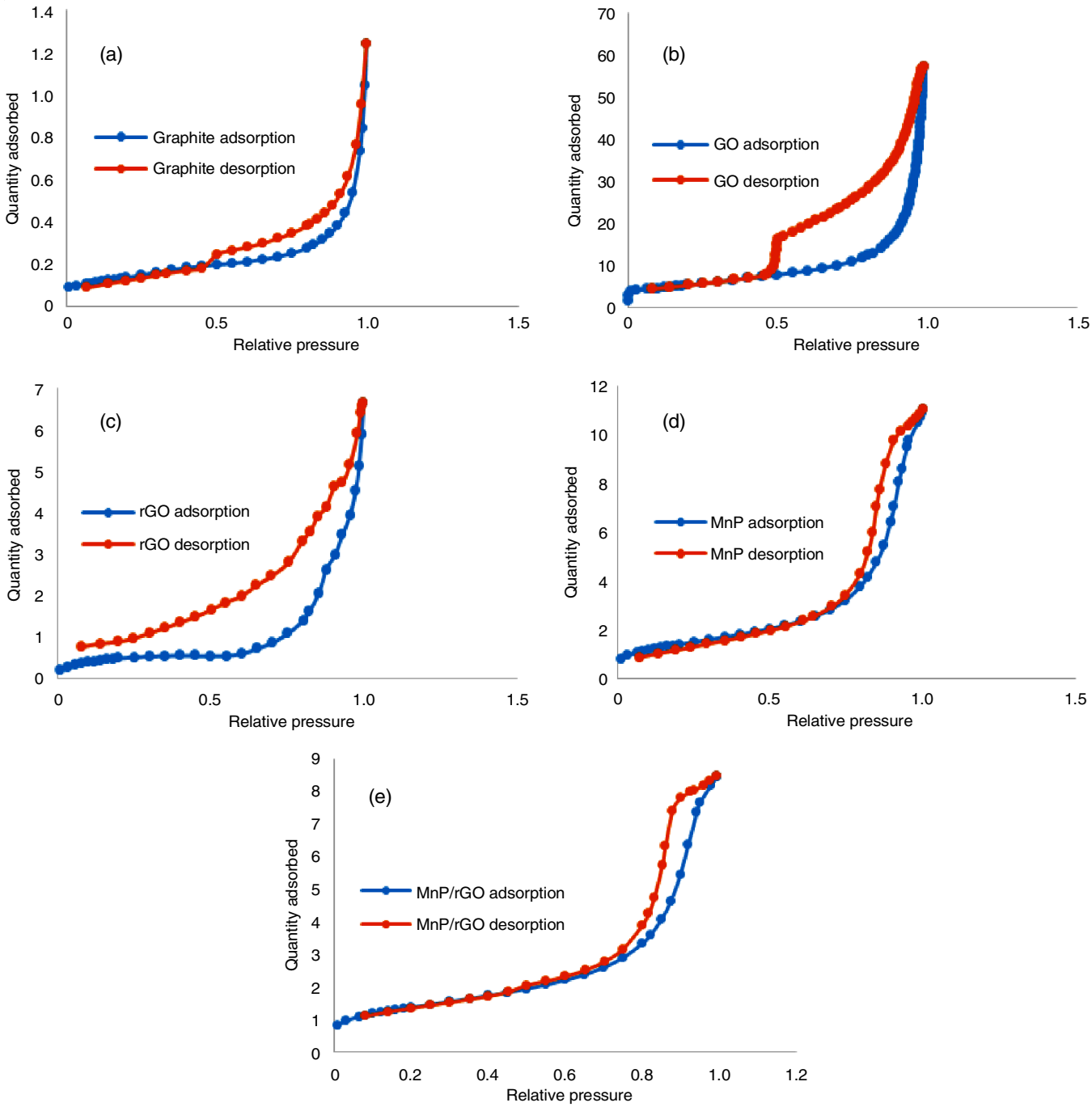

Fig. 4. Isotherm linear plot of (a) graphite, (b) GO, (c) rGO, (d) Fe_3O_4 and (e) Fe_3O_4/rGO

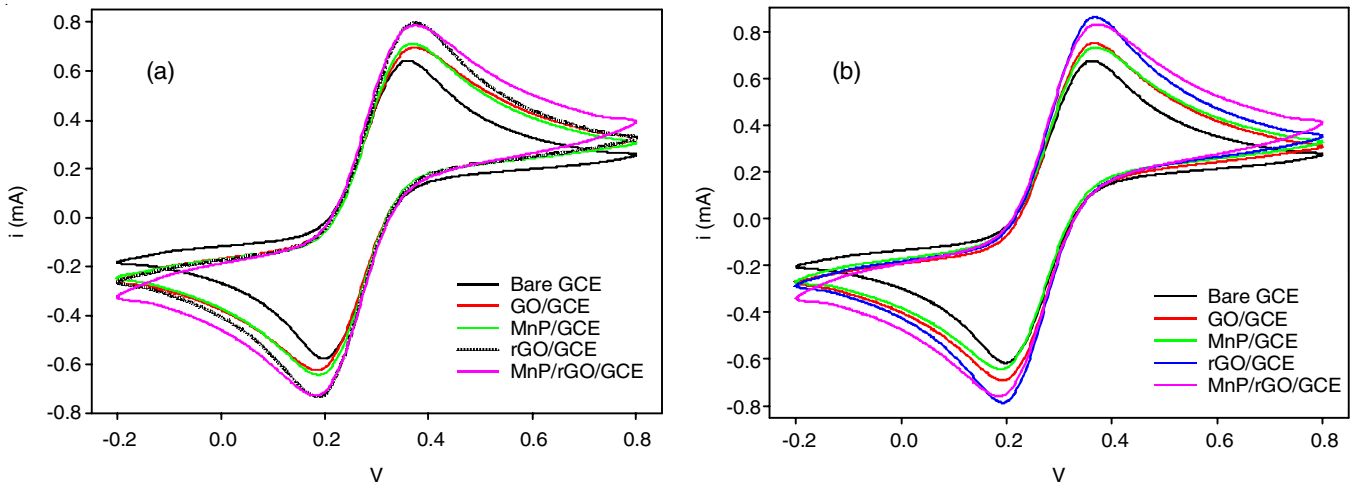

Fig. 5. Cyclic voltammogram of the response of modified electrode in (a) electrolyte of KCl and $K_4[Fe(CN)_6]$ and (b) electrolyte of standard dopamine with PBS solution as supporting electrolyte

studied using cyclic voltammetry technique to verify the best electrode that has excellent electron transfer property in the supporting electrolyte of KCl and $K_4[Fe(CN)_6]$. Fig. 5a shows that the redox peak current of modified GCE is more define compared to the bare GCE. This signifies that the presence of composite onto the GCE provide distinguished electron transfer between the redox probe and electrode surface. High electron transfer also can associate with the high electrical conductivity of the composite on the surface of electrode [13]. The data show that Fe_3O_4/rGO/GCE has the lowest peak separation (Table-2), which it undergoes a completely reversible process compared to other electrodes [14].

A cyclic voltammetry technique was used to determine the performance of each modified GCE and bare GCE in standard dopamine. The high electron transfer characteristic of the best modified electrode will be chosen to determine dopamine in the real sample. The resulting voltammogram shows that the modified electrode of Fe_3O_4/rGO/GCE gives the best performance even when detecting dopamine standard in the supporting electrolyte of KCl and $K_4[Fe(CN)_6]$. The anodic peak current of Fe_3O_4/rGO/GCE (Fig. 5b) gives a value of 0.8 µA while the anodic peak current of Fe_3O_4/rGO/GCE in Fig. 5b) gives a value of 0.771 µA. The peak potential (0.35 V to 0.40 V) of voltammogram do not shift much compared to the modified electrode without dopamine standard in the electrolyte (Fig. 5a), which shows that the electrode has the same response towards the redox reaction of analyte [15]. The anodic and cathodic peak current is increasing compared to the electrochemical characterization with the absence of dopamine in the electrolyte (Fig. 5a), which display that the electrode has a reaction towards the analyte present in the electrolyte.

The experimental EIS was performed in a frequency range of 100 kHz to 100 mHz and the resulting Nyquist plot and the bode phase plot of bare GCE and modified GCE is shown in Fig. 6. Based on the Nyquist plot of bare GCE and modified GCE (Fig. 6), the interfacial electron transfer resistance exists in bare GCE, GO/GCE and Fe_3O_4/GCE which implied by the curve of resistance of bare GCE, GO/GCE and Fe_3O_4/GCE but it do not shows its characteristic of curve on the plot of Fe_3O_4/rGO/GCE [16,17]. The modified electrode of Fe_3O_4/rGO/GCE display the smaller resistance between the redox active species and the electrode surface and enhance the performance of electron exchange. The charge transfer resistance of bare GCE, Fe_3O_4/GCE and GO/GCE is high compared to Fe_3O_4/rGO/GCE charge transfer resistance [18].

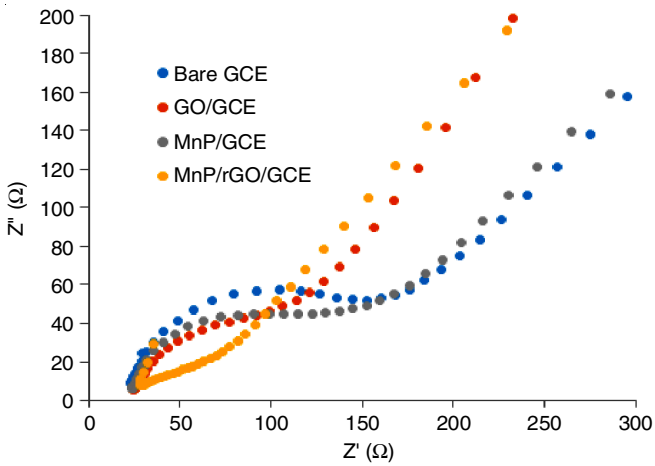

Fig. 6. Nyquist plot of bare GCE and modified GCE with KCl and $K_4[Fe(CN)_6]$ act as supporting electrolyte

TABLE-2
DIFFUSION COEFFICIENTS AND PEAK SEPARATION VALUE OBTAINED FOR THE EFFECT OF SCAN RATE RANGE FROM 50 to 250 mV s^{-1}

Scan rate (mVs^{-1})	Anodic potential sweep, E_{ap} (V)	Cathodic potential sweep, E_{cp} (V)	Peak separation, ΔE_p (V)	Anodic peak current (A)	Diffusion coefficient (cm^2/s)
50	0.36	0.26	0.10	1.29×10^{-5}	9.01×10^{-17}
100	0.39	0.23	0.16	1.94×10^{-5}	1.02×10^{-16}
150	0.41	0.21	0.20	2.56×10^{-5}	1.18×10^{-16}
200	0.43	0.20	0.23	3.02×10^{-5}	1.23×10^{-16}
250	0.44	0.18	0.26	3.42×10^{-5}	1.27×10^{-16}

Optimization parameters: To obtain the best condition for the analysis, several parameters have been chosen which are scan rates of the cycle, the concentrations of analyte and the pH of electrolyte. The selected range of scan rate varies from 50 mV s^{-1} to 250 mV s^{-1}. With constant and standardized scan cycle of six cycles, the concentration of 100 µM and potential range from – 0.2 V to 0.8 V.

Fig. 7 shows the voltammogram obtained for the effect of scan rate on Fe_3O_4/rGO/GCE in standard dopamine. It shows the linear relationship between the scan rate and the current obtained. This result implied that the electrochemical oxidation was an absorption-controlled process for dopamine which might be owing to the effective π-π conjugation between the aromatic moieties of dopamine and the modified electrode of Fe_3O_4/rGO/GCE [19]. The defined peak current of 250mV s^{-1} was chosen as the optimized scan rate as the linear relationship of the peak current and the applied potential give the best result of highest scan rate. The scan rate of 250mV s^{-1} also gives the high value of peak separation which is near the ideal peak separation of ~59 mV s^{-1} and small diffusion layer deposited on the surface of electrode thus enhance the electron transfer between the redox species of dopamine and the electrode. In high scan rate, the diffusion layer onto the surface of electrode became smaller due to the applied potential.

Ten different concentrations of dopamine standard were evaluated to determine the best concentration that will give the highest and sharp peaks in the cyclic voltammetry (Fig. 8a). The concentration's range to be valued in the experiment is from 20, 40, 60, 80, 100, 120, 140, 160, 180 and 200 µM. With constant rate, the increase of dopamine concentration will increase the amount of electro-active species that can enhance the electron transfer on the electrode surface. This demonstrates that the concentration of dopamine is proportional to electron transfer between redox species and electrode and thus proportional to the peak current obtained. The anodic peak current value of the cyclic voltammogram increases from low concentration to high concentration.

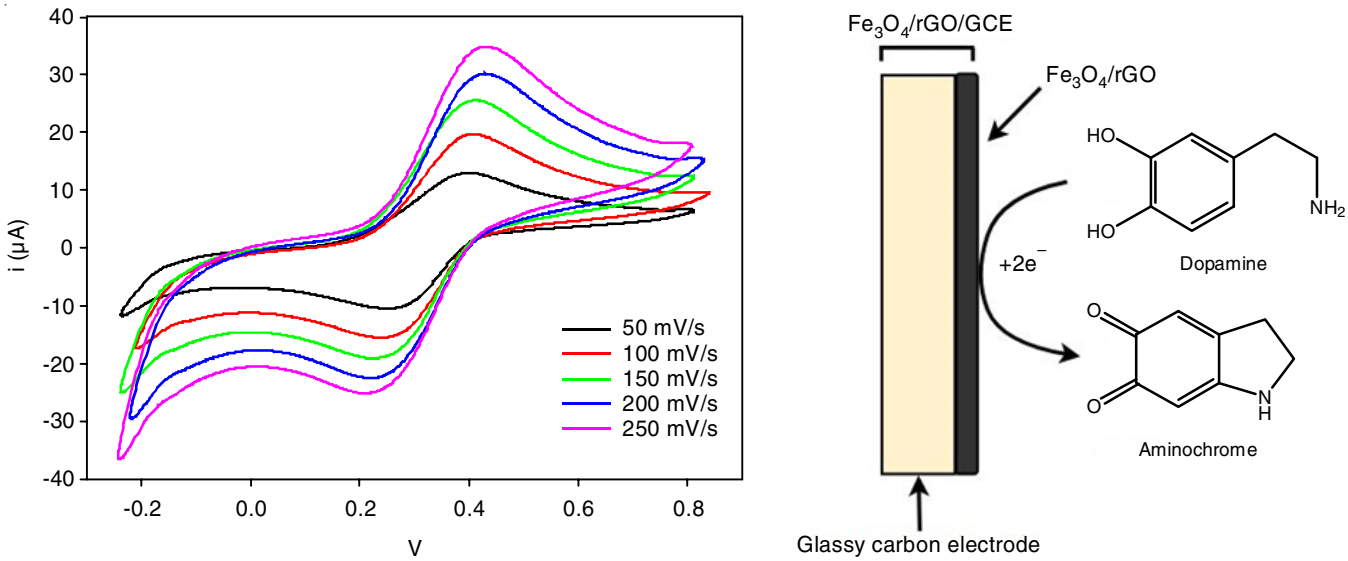

Fig. 7. Effect of scan rate on the cyclic voltammetry with 0.1 mol/L KCl and 2.0 mmol/L $K_4[Fe(CN)_6]$ as the supporting electrolyte at different scan rate of 50 mV/s until 250 mV/s

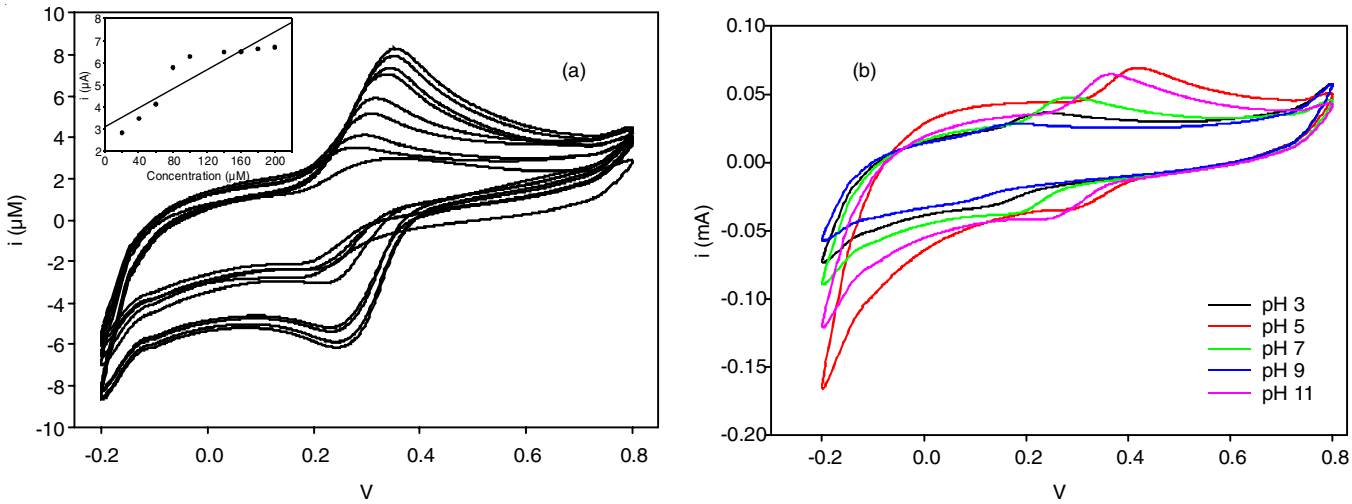

Fig. 8. Cyclic voltammogram of (a) effect of concentration in DA solution from 20 µM until 200 µM in supporting electrolyte of 0.1 M PBS solution (pH 7.0). Inset: Calibration curve of anodic peak current *versus* concentration of dopamine used in the solution and (b) effect of pH varies from pH 5 to pH 11 in 0.1 M PBS solution

The pH ranges from acidic medium which are pH 3 and pH 5, neutral medium (pH 7) to alkaline pH of 9 and 11 were investigated to know the behaviour of dopamine in the acidic, neutral and basic medium. Cyclic voltammogram of the effect of pH (Fig. 8b) shows that dopamine gives an optimum performance at pH 7. The optimum pH is chosen from the oxidation peak current nearly potential of zero with define and sharp peak. From Fig. 8b, the peak current of dopamine standard in acidic medium is shifted to the potential near zero but in acidic medium, the electrode cannot detect dopamine due to high H^+ charge in the electrolyte thus, the peak of dopamine is not sharp in the voltammogram. While in the basic medium, the peak is defined but far from the zero potential which indicate the modified electrode of Fe_3O_4/rGO/GCE did not couple with dopamine standard in the electrolyte [15].

Validation parameters: The real sample used for this project is urine samples from human as dopamine is mostly being discharged through urine. The urine of a healthy person is being collected and preserved using a specific method and run for the validation parameters of a limit of detection, limit of quantification, recovery study, repeatability and reproducibility. Determination of dopamine level in urine real sample is crucial to discover the practicability of modified electrode Fe_3O_4/rGO/GCE.

Limit of detection is the lowest amount of analyte which in this study is dopamine, in a real sample which can be detected but it is not necessarily quantitated as an exact value. For this study, the method based on standard deviation of the slope was used as this approach provide the simplest method of calculation by using eqn. 1a from the calibration curve of effect of concentration. The quantification limit of an individual analytical procedure is the lowest amount of analyte in a sample which can be quantitatively determined with suitable precision and accuracy. The quantification limit is a parameter of quantitative assays for low levels of compounds in sample matrices and is used particularly for the determination of impurities and/or degradation products [2].

$$\text{LOD} = \frac{3 \times \text{Standard error}}{\text{Slope}} \quad (1a)$$

$$\text{LOQ} = \frac{10 \times \text{Standard error}}{\text{Slope}} \quad (1b)$$

For a linear calibration curve, it is assumed that the instrument response y is linearly related to the standard concentration x for a limited range of concentration [4]. Both the LOD and LOQ values (Table-3) show the excellent detection limit of dopamine determination in human urine sample compared to the conventional method of chromatographic and spectroscopy technique.

A recovery study was carried out to determine the effectiveness of the method. Recovery can be defined by the fraction of the analyte determined after addition of a known amount of the analyte to a sample [20]. In this study, a urine sample has been treated with acetic acid was used as the controlled unspiked sample. The unspiked samples as well as the spiked sample with dopamine standard, were analyzed three times. The averaged result and the relative standard deviation (RSD) was obtained and calculated (Table-4). The amount and percent recovered from the sample was calculated using eqn 2:

TABLE-3
LOD AND LOQ OBTAINED FOR THE DOPAMINE CONCENTRATION

	LOD	LOQ
Coefficient value	39.653	39.653
Standard error	7.523	7.523
Value obtained	0.569 μM	1.897 μM

$$\text{Recovery} = \frac{\text{Mass of spiked sample (g)} - \text{Mass of unspiked sample (g)}}{\text{Mass of spiked standard (g)}} \quad (2)$$

Reproducibility is the measure of agreement between results obtained with the same method on the identical test or reference material under different conditions (by different persons, in different laboratories, with different equipment and at different times) [21]. In this work, the urine sample from three different individuals was taken and analyzed on the same day to ensure the result of reproducibility is reliable. The analysis was done using differential pulse voltammetry technique and the relative standard deviation was calculated by using eqn 3:

$$\text{Relative standard deviation (\%)} = \frac{\text{Standard deviation}}{\text{Mean}} \times 100 \quad (3)$$

The reproducibility value obtained for the RSD is 7.19% which satisfy the desired percentage for below than 20 %. The results proposed that the modified electrode of Fe_3O_4/rGO/GCE possess the property of reproducibility and high stability but non-repeatable (Table-5). The modified electrode is suitable for the detection of the biological matrix but the analysis of the sample has drawbacks which cannot be repeated at using the same composite cast on GCE.

TABLE-5
DATA OBTAINED FOR REPRODUCIBILITY PERCENTAGE

	Reproducibility
Mean	1.834×10^{-5}
Standard deviation	1.319×10^{-6}
Relative standard deviation (%)	7.19

Conclusion

The modified electrode of Fe_3O_4/rGO/GCE has been successfully synthesized by a simple and low-cost technique with an environmentally friendly approach *via* a facile one-step synthetic route. The graphene-based nanocomposite exhibits excellent

TABLE-4
RECOVERY RESULT FOR THE THREE SUCCESSIVE URINE REAL SAMPLE

Real samples	Current for unspiked sample (A)	Mass of unspiked sample (g)	Current for spiked sample (A)	Mass of spiked sample (g)	Recovery (%)
1	3.658×10^{-7}	0.000135	6.931×10^{-6}	0.003201	113
2	1.648×10^{-7}	0.000148	2.936×10^{-6}	0.000432	105
3	1.541×10^{-7}	0.000149	1.035×10^{-6}	0.000385	87

and unique properties of catalytic properties and electronic behaviour. The electrochemical behaviour and characterization using cyclic voltammetry technique and electron impendance spectroscopy showed that the modified GCE of Fe_3O_4/rGO/GCE exhibit an improved peak separation and electron transfer properties towards the redox reaction of dopamine compared to bare GCE. The charge transfer resistance for the modified electrode is low which indicate the resistance between the electrode probe and the electrolyte is low in comparison to bare GCE. The composite of Fe_3O_4/rGO was investigated by various characterization methods and the result prove that Fe_3O_4/rGO/GCE has been successfully synthesized. The Fe_3O_4/rGO/GCE sensor electrode exhibit a characteristic of high recovery, reproducibility, low detection limit and low limit of quantitation of 113-87 %, 7.19 %, 0.569 µM and 1.897 µM, respectively for the analysis of real samples. These results reveal that Fe_3O_4/rGO/GCE is a potential candidate for the platform of biosensor and electrochemical applications compared to the conventional method for sensing of dopamine.

ACKNOWLEDGEMENTS

The authors gratefully acknowledge to Ministry of Education for financial support from the Fundamental Research Grant Scheme (FRGS)FRGS/1/2017/STG01/UMT02/2 and Central Lab UMT for providing facilities for undertaking this research.

CONFLICT OF INTEREST

The authors declare that there is no conflict of interests regarding the publication of this article.

REFERENCES

1. M.Z.H. Khan, *J. Nanomater.*, **2017**, Article ID 8178314 (2017); https://doi.org/10.1155/2017/8178314.
2. A. Pandikumar, G.T. Son How, T.P. See, F.S. Omar, S. Jayabal, K.Z. Kamali and N.M. Huang, *RSC Adv*., **4**, 63296 (2014); https://doi.org/10.1039/C4RA13777A.
3. B.J. Verton and R.M. Wightman, *Anal. Chem*., **75**, 414A (2003); https://doi.org/10.1021/ac031421c.
4. Y. Shao, J. Wang, H. Wu, J. Liu, I.A. Aksay and Y. Lin, *Electroanalysis*, **22**, 1027 (2010); https://doi.org/10.1002/elan.200900571.
5. M. Zhou, Y. Zhai and S. Dong, *Anal. Chem*., **81**, 5603 (2009); https://doi.org/10.1021/ac900136z.
6. Wahajudin and S. Arora, *Int. J. Nanomed*., **7**, 3445 (2012); https://doi.org/10.2147/IJN.S30320.
7. H.J. Jung, B.W. Kim, M.A. Malek, Y.S. Koo, J.H. Jung, Y.S. Son and C.U. Ro, *J. Hazard Mater.*, **213-214**, 331-340 (2012); https://doi.org/10.1016/j.jhazmat.2012.02.006.
8. S. Park and R.S. Ruoff, *Nat. Nanotechnol*., **4**, 217 (2009); https://doi.org/10.1038/nnano.2009.58.
9. V. Chandra, J. Park, Y. Chun, J.W. Lee, I.C. Hwang and K.S. Kim, *ACS Nano.*, **4**, 3979 (2010); https://doi.org/10.1021/nn1008897.
10. P.K. Chu and L. Li, *Mater. Chem. Phys*., **96**, 253-277 (2006); https://doi.org/10.1016/j.matchemphys.2005.07.048.
11. J. Chen, B. Yao, C. Li and G. Shi, *Carbon*, **64**, 225 (2013); https://doi.org/10.1016/j.carbon.2013.07.055.
12. K. Sing, *Colloids Surf.: A Physiochem. Eng. Asp*., **187-188**, 3 (2001); https://doi.org/10.1016/S0927-7757(01)00612-4.
13. N. Elgrishi, K.J. Rountree, B.D. McCarthy, E.S. Rountree, T.T Eisenhart and J.L. Dempsey, *J. Chem. Educ*., **95**, 197 (2018); https://doi.org/10.1021/acs.jchemed.7b00361.
14. R.S. Nicholson and I. Shain, *Anal. Chem*., **36**, 706 (1964); https://doi.org/10.1021/ac60210a007.
15. A.J. Arvia, S.L. Marchiano and J.J. Podesta, *Electrochim. Acta*, **12**, 259 (1967); https://doi.org/10.1016/0013-4686(67)80004-5.
16. F. Yusoff, N. Mohamed, A. Aziz and S.A. Ghani, *Mater. Sci. Appl*., **5**, 199 (2014); https://doi.org/10.4236/msa.2014.54025.
17. N.B. Muhamad, W.M. Khairul and F. Yusoff, *J. Solid State Chem*., **275**, 30 (2019); https://doi.org/10.1016/j.jssc.2019.04.003.
18. Y.J. Ren, M.R. Anisur, W. Qiu, J.J. He, S. Al-Saadi and R.K. Singh Raman, *J. Pow. Sourc.*, **362**, 366 (2017); https://doi.org/10.1016/j.jpowsour.2017.07.041.
19. Q. Lian, Z. He, Q. He, A. Luo, K. Yan, D. Zhang and X. Zhou, *Anal. Chim. Acta*, **823**, 32 (2014); https://doi.org/10.1016/j.aca.2014.03.032.
20. A. Shrivastava and V.B. Gupta, *Chron. Young Sci*., **2**, 21 (2011); https://doi.org/10.4103/2229-5186.79345.
21. T. Peik-See, A. Pandikumar, H. Nay-Ming, L. Hong-Ngee and Y. Sulaiman, *Sensors*, **14**, 15227 (2014); https://doi.org/10.3390/s140815227.